Selective excitation of erbium in silicon-infiltrated silica colloidal photonic crystals

J. Kalkman,[a] E. de Bres, and A. Polman
FOM Institute for Atomic and Molecular Physics, Kruislaan 407, 1098 SJ Amsterdam, The Netherlands

Y. Jun and D. J. Norris
Department of Chemical Engineering and Material Science (CEMS), University of Minnesota, Minneapolis, MN 55455-0132

D. C. 't Hart, J. P. Hoogenboom, and A. van Blaaderen
Department of Soft Condensed Matter, Debye Institute, Utrecht University, Princeton Plein 5, 3584CC Utrecht, The Netherlands

(Received 16 September 2003; accepted 18 November 2003)

Optically active erbium ions in the silica and silicon sections of a Si-infiltrated silica colloidal photonic crystal can be separately addressed. A face-centered cubic colloidal crystal composed of 860 nm silica colloids was made by self-assembly under controlled drying conditions. It was then infiltrated with Si using chemical vapor deposition at 550 °C. Next, the photonic crystal was doped with erbium ions by 2 MeV ion implantation. The erbium ions were activated by thermal anneals at 400 and 750 °C, and showed clear photoluminescence at 1.5 μm in both the Si and silica parts of the photonic crystal. By varying measurement temperature and excitation wavelength the erbium ions were selectively excited in Si and/or silica. In this way the local optical density of states in these photonic crystals can be selectively probed. The emission linewidth for Er^{3+} in crystalline Si is relatively narrow and fits well within the calculated photonic band gap. The long luminescence lifetime of Er in Si makes these photonic crystals an ideal geometry to measure effects of the optical density of states on spontaneous emission. © *2004 American Institute of Physics.*
[DOI: 10.1063/1.1640459]

I. INTRODUCTION

The spontaneous emission rate of an atom is not only a property of the atom, but also depends on the density of states (DOS), a property determined by the atom's dielectric environment.[1,2] Recently, with the introduction of the concept of photonic crystals (PCs),[3–5] it has been predicted that it will be possible to make materials with a photonic band gap (PBG). Photonic crystals are materials that consist of a regular arrangement of dielectric material that interact strongly with light. When properly designed, a PC exhibits a frequency range where, for all wave vectors, the DOS vanishes and no electromagnetic modes are allowed. If the emission frequency of an atom falls within such a forbidden frequency range (the photonic band gap) the spontaneous emission is completely inhibited. It is a great challenge to fabricate these PCs with a PBG at optical and near-infrared frequencies, and to show a significant effect on the spontaneous emission rate. So far, no large effect on the spontaneous emission rate has been successfully demonstrated in PCs. In several studies on spontaneous emission the PCs do not possess high-enough refractive-index contrast to have a PBG.[6] In another study,[7] for a Si PC, which does posses high-enough index contrast, a large change in the spontaneous emission spectrum was achieved, but the crystal was too thin to observe a large effect on the emission rate.

In this article we present the fabrication of an erbium-doped face-centered cubic (fcc) Si-inverted opal PC that has high-enough index contrast and sufficient thickness so that the effect of the PBG on the spontaneous emission may be observed. To fabricate this structure, a crystal is grown from silica colloids by self-assembly. The colloidal crystal is then infiltrated, after which the colloids are removed, so that an air-sphere crystal remains. This concept was demonstrated for infiltration with TiO_2,[8,9] and recently, infiltration with Si was demonstrated.[10,11] An air-sphere opal, with fcc symmetry, fully infiltrated with Si has a PBG between the eighth and ninth band of 4.25% of the center frequency,[12] the latter being determined by the crystal's lattice parameter. Structures that are not fully infiltrated can posses band gaps that are even larger, up to 8%.[12] Recently, a technique was developed in which large-area colloidal crystals were grown on a Si substrate.[11] The planar geometry of these crystals makes it possible to use thin-film techniques such as ion implantation to incorporate optical dopants into the PC.

We use Er ions as optical probes in a Si-infiltrated silica colloidal crystal. Erbium is a rare-earth atom that takes on a trivalent state in a solid, and shows intra-4f transitions at 1.5 μm. The use of Er as an optical probe has several advantages over dyes; Er shows a narrow emission line width and it does not photo bleach, a problem frequently encountered with dyes. When incorporated in either Si or silica Er can be made optically active by thermal annealing. The 1.5 μm Er emission energy is smaller than the Si band-edge energy, and,

[a]Author to whom correspondence should be addressed; electronic mail: kalkman@amolf.nl

therefore, the Si host does not absorb the Er emission. After etching out the silica colloids, the index contrast increases [at 1.5 μm, $n=3.5$ (crystalline Si) and $n=3.59$ (amorphous Si)] and a PC is made that, according to calculations,[12] has a PBG. The goal of this article is to demonstrate the fabrication of an Er-doped fcc Si-inverted opal PC and to investigate the intrinsic optical properties of such a crystal. We do so by fabricating a PC with a PBG that does not overlap with the Er emission spectrum and dope only the near-surface region of the PC, so that photonic effects on the Er emission are small. These data serve as a reference for future experiments were Er is placed inside a PC with a PBG at 1.5 μm. In our experiments Er is optically activated in both Si and silica host materials, and, by changing the experimental conditions, Er ions can be selectively excited in Si and/or silica. We find that the Er emission line width matches well with the PBG calculated for an fcc Si-inverted opal with the proper lattice constant.

II. FABRICATION, STRUCTURAL AND OPTICAL CHARACTERIZATION

We used the Stöber method[13] to grow silica colloids from tetra-ethoxy-silane (TEOS). Small-size nuclei were grown first, and, subsequently, their diameter was increased to 860 nm by adding (under well-controlled conditions) additional TEOS to the solution.[14] The amount of dumbbells in the solution was below 1%, and the resulting size polydispersity was 2.5%. By controlled drying,[15] a colloidal crystal was grown on a Si substrate, which was mounted at an angle of 80° in a vial, filled with a 1 vol % colloidal suspension. The solvent evaporated by keeping the vial at 70 °C in a hot-air oven. The capillary forces at the retreating meniscus causes the self-assembly of an fcc colloidal crystal on the Si substrate. We investigated the colloidal crystal quality with scanning electron microscopy (SEM) and observed a maximum domain size of ~100 μm and a crystal thickness of ~15 layers of colloids. Figure 1(a) shows the fcc (111) surface plane of the colloidal crystal after self-assembly by controlled drying. The inset shows the Fourier transform of an image covering an area of 100 μm×60 μm, demonstrating the long-range order we achieved for these samples.

The colloidal crystals were infiltrated with Si by means of low-pressure chemical-vapor deposition with silane.[11] The samples were heated to 550 °C and, over the course of 3 h, infiltrated with Si while the silane pressure, and gas-flow rate, were kept at 743 mTorr and 90 sccm, respectively. The infiltration resulted in an almost complete filling of the interstices of the colloidal crystal with amorphous-Si (a-Si) and the deposition of an a-Si layer on top of the crystal. The a-Si top layer was removed using an SF_6 reactive-ion etch. Since SF_6 etches Si selectively, the silica colloids act as an etch stop for the Si etch. Etching was stopped when the silica colloids were exposed on the surface [see Fig. 1(b)].

Next, the samples were implanted with 2.05 MeV Er^{2+} ions, resulting in a Gaussian depth distribution. The implanted fluence was measured on a Si reference sample by Rutherford backscattering spectrometry and amounted to 2.5×10^{14} Er/cm^2. Note that the erbium ions are distributed in both the Si and the silica part of the PC. The ion range and

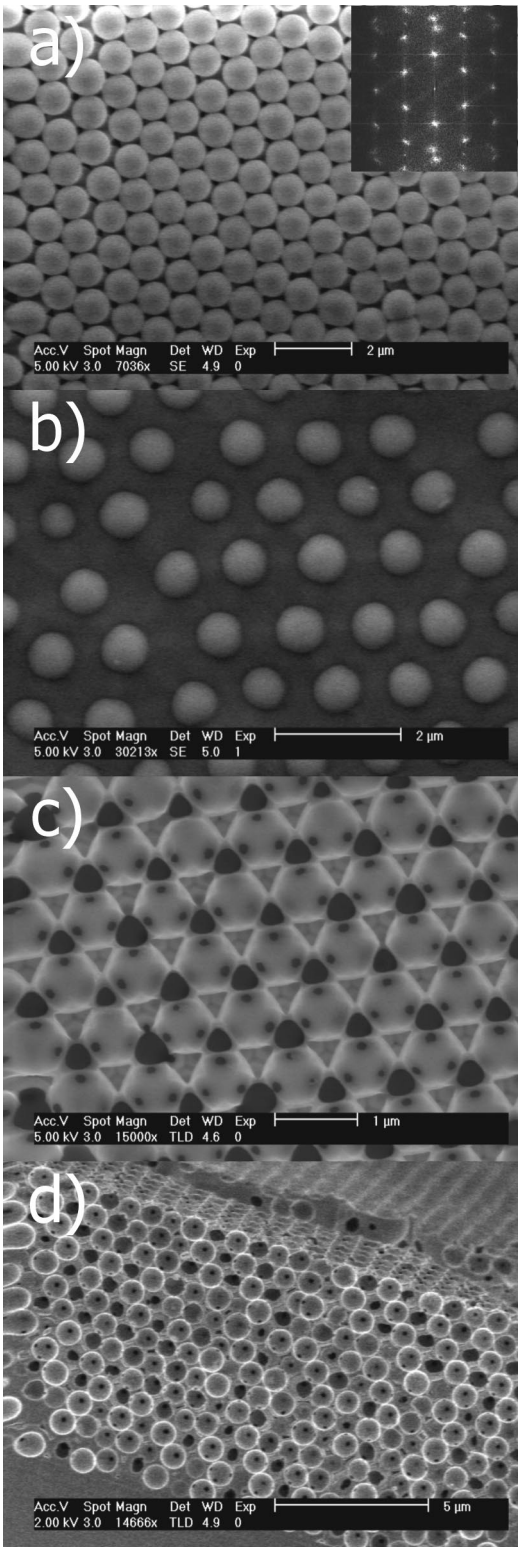

FIG. 1. SEM micrographs of the various stages in the fabrication process of the Si inverted opal PC: (a) fcc (111) plane at the top of the colloidal crystal, which was grown by controlled drying. The inset shows the Fourier transform of a large-area image, indicating long-range crystal order; (b) Si infiltration and dry etching results in a well-defined crystal plane on top of the crystal; (c) same top view, but after HF etching, which creates the inverted-opal structure by etching out the silica all the way to the substrate; (d) fcc (110) plane of the same sample, showing the cross section of the crystal. Note the almost complete filling of the interstices of the original colloidal crystal.

straggle for this energy are $\mu=640$ nm, $\sigma=128$ nm for Si, and $\mu=533$ nm, $\sigma=106$ nm for colloidal silica, respectively. To increase the index contrast, and thus create a PC with a PBG, the silica was etched out by immersing the sample in a 5.5 wt. % buffered HF solution (buffered with NH_4F) for 8 min. Figure 1(c) shows a top view of the etched sample. The small holes in the air spheres are the points where the silica colloids originally touched. This connectedness of the air network is first of all essential in order for the reaction products to be able to leave the sample. Moreover, it leads to a larger band gap.[16] On a larger scale than shown in Fig. 1(c) cracks are visible that are the result of shrinkage of the colloids during Si infiltration. These cracks are filled with Si. The typical domain size after infiltration is ~20 μm. Figure 1(d) shows a view of the (110) lattice plane after cleaving. It shows that the crystallinity is maintained through the full cross section of the crystal. Also, it can be seen that the silica colloids were etched out all the way through to the bottom of the sample.

We performed temperature-dependent photoluminescent (PL) spectroscopy measurements by mounting the samples in a closed-cycle He cryostat. The Er^{3+} ions were excited with an acousto-optically time-modulated Ar ion laser, operated at a power of 10 mW. PL was collected with an $f=15$ cm lens, dispersed with a 480 mm focal-length monochromator, and detected with a liquid-nitrogen-cooled Ge detector in combination with a lock-in amplifier. Decay and excitation rates were obtained by averaging the time-dependent PL signal, after switching the laser beam off and on, respectively.

We made spectrally resolved far-field optical reflectivity measurements (not shown), with the incident beam under an angle of 17° with respect to the surface normal, to investigate the optical properties of the Si-inverted opal PC with the silica etched out. The as-deposited sample showed peaks at 1600 and 1200 nm, attributed to stopgaps between the fourth and the fifth band, and the eighth and ninth band, respectively. Upon annealing at 750 °C the peaks shifted to smaller wavelengths. We attribute this to the crystallization of the silicon that was initially deposited in its amorphous state. We measured the refractive index, which changed from 3.59 (amorphous Si) to 3.5 (crystalline Si) upon annealing. The crystallization was confirmed by Raman measurements that showed a change from a broad Raman spectrum, characteristic of *a*-Si, to a spectrum composed of a single peak indicating the crystallization of the Si. The reflectivity spectra showed peak reflectivities on the order of 6%–8%, well below the values close to 100% observed earlier on a similar crystal.[17] This is attributed to the fact that in these particular samples the presence of multiple domains and grain boundaries reduces the specular reflectivity. Note that effects on spontaneous emission, in these photonic crystals with relatively high index contrast, are mostly determined by medium- and short-range order in the crystal and thus large-scale disorder should not be considered a major problem in studies on modified spontaneous emission.

III. RESULTS AND DISCUSSION

To characterize optically active Er^{3+} ions in *a*-Si we annealed an Er-implanted Si-infiltrated colloidal crystal (silica not etched out) for 1 h at 400 °C in vacuum. Figure 2 shows the PL spectra, taken at temperatures in the range of 20–200 K under excitation at $\lambda=488$ nm. A broad emission spectrum, with a full width at half maximum (FWHM) of 29 nm, can be observed, a feature that is mainly caused by inhomogeneous broadening due to the varying nearest neighbor surrounding the Er^{3+} ions in the amorphous Si matrix. The PL peak intensity quenched by a factor of 10 when the temperature increased from 20 to 200 K. Time-dependent PL measurements of the decay rate were performed and showed a $1/e$ decay time of 300 μs, independent of PL temperature. PL decay measurements did not show any contribution from Er^{3+} in silica (which should have a lifetime in the ms range), which is consistent with earlier work that showed that activation of Er^{3+} in silica colloids occurs only for anneal temperatures above 700 °C.[18] As has been seen before,[19] Er^{3+} in *a*-Si can be excited through photons at energies larger than the electronic *a*-Si band edge energy. These photons generate photocarriers that can become trapped at an erbium-related trapping site, where they recombine and induce excitation of the Er^{3+} ions through an impurity Auger process. Quenching of the PL intensity with temperature can occur as a result of a reduced excitation efficiency, or due to backtransfer, which is the transfer of energy from an excited Er^{3+} ion back to the trapping site.[20,21] The fact that the PL lifetime is temperature independent indicates that the decrease in PL with increasing temperature is not due to backtransfer.

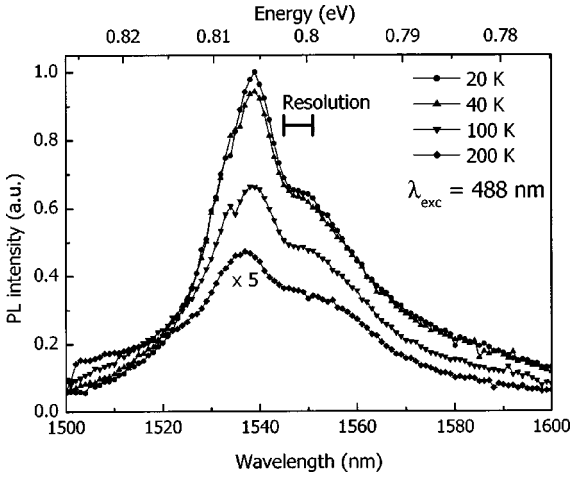

FIG. 2. PL spectra of an Er-implanted silicon-infiltrated colloidal crystal after annealing at 400 °C. Spectra are taken at different temperatures. The broad spectrum and the PL quenching with increasing temperature are characteristic features for Er in *a*-Si. Pump wavelength is 488 nm.

We note that earlier work[22] has shown that Er^{3+} shows no PL in pure *a*-Si. Our later work[19] has shown that passivation of defects by hydrogen, and the presence of small amounts of oxygen, are essential to activate Er^{3+}. We can therefore conclude that the chemical vapor deposition infiltration process includes these impurities in the *a*-Si matrix. Next, we investigate the quenching and excitation mechanisms of Er^{3+} in a Si-infiltrated colloidal crystal annealed for 1 h at 750 °C, which leads to the crystallization of *a*-Si and optical activation of Er^{3+} in silica. Figure 3 shows the PL spectra of this sample, measured at temperatures in the range

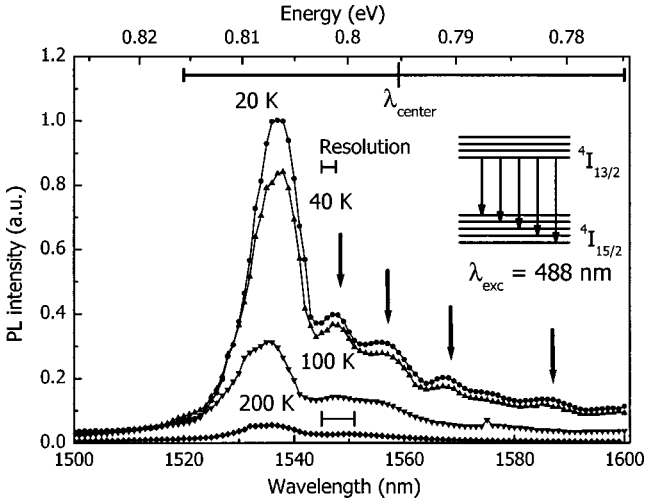

FIG. 3. PL spectra of an Er-implanted silicon-infiltrated colloidal crystal after annealing at 750 °C (resolution for 20 and 40 K, 2.6 nm, other temperatures 6 nm, see resolution bars). The excitation wavelength was 488 nm. The PL spectra at 20 and 40 K show Stark splitting due to the crystal field of *c*-Si, as indicated by the arrows. The inset shows a schematic of the Stark splitting of the energy levels and transitions that result in the observed spectral shape. The PL intensity decreases for increasing temperature. This is ascribed to a detrapping process that reduces the excitation efficiency. The scale bar on top shows the calculated wavelength range of the PBG for a fcc Si inverted opal PC with a lattice parameter of 1237 nm.

of 20–200 K, and excited at a wavelength of 488 nm. Again, strong PL quenching with increasing temperature is observed, a known effect for Er^{3+} in crystalline Si (*c*-Si).[23] For the measurements at 20 and 40 K, a narrow main emission peak is observed (FWHM=11 nm). Moreover, several pronounced peaks, indicated by arrows, can be seen in the PL spectra. This structure is caused by Stark splitting of degenerate $4f$ energy levels of Er^{3+}, due to the crystal field around the atom.[24] The asymmetry in the spectrum is caused by the fact that at these measurement temperatures only the lowest level in the first excited state manifold ($^4I_{13/2}$) is populated. Therefore, only emission lines at the long-wavelength side of the main emission peak are observed. From the observation of the Stark levels, we can assume that the Er^{3+} ions are in a crystalline environment. This is in agreement with the high anneal temperature, which is known to cause crystallization of erbium-doped *a*-Si.[25] In these experiments an excitation wavelength of 488 nm was chosen, which causes excitation of Er^{3+} in silica by direct optical excitation into the $^4F_{7/2}$ manifold, and in *c*-Si by a photocarriers mediated process. To determine the relative PL contribution of Er^{3+} from either one of the host materials, we measured the time-dependent PL decay at 1.536 μm for temperatures in the range of 20–200 K. Figure 4 shows normalized PL decay traces. At 200 K the PL decay shows a long lifetime (7 ms), characteristic for Er^{3+} in silica.[26] At this temperature the PL from Er^{3+} in *c*-Si is fully quenched. The spectrum in Fig. 3 measured at 200 K, therefore only originates from Er^{3+} in silica. At lower temperatures a fast PL decay component appears with a lifetime of 0.9 ms, characteristic for Er^{3+} in *c*-Si.[27] Since this lifetime is similar to the longest lifetime observed for Er-implanted *c*-Si, it is most likely close to the radiative lifetime. The assumed high quantum efficiency makes this Er-doped Si-inverted opal PC an ideal geometry to measure the effects of the optical DOS on the spontaneous emission lifetime. A biexponential fit to the PL decay at 20 K yields the relative contributions of Er^{3+} in *c*-Si and silica to the PL: 78% and 22%, respectively. As the volume fractions of Si and silica are 26% and 74%, respectively, this indicates that for a given pump power PL from Er^{3+} is more efficiently excited in Si than in silica. This is attributed to the large cross section for the generation of photocarriers in *c*-Si that subsequently couple to Er^{3+}, compared to the relatively small cross section for direct excitation of Er^{3+} in silica.

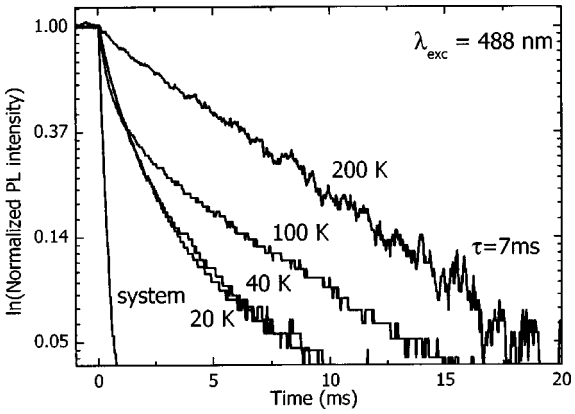

FIG. 4. Normalized PL decay measurements, taken at 1.536 μm at different temperatures (see for spectra Fig. 3). After excitation at 488 nm the laser is switched of at $t=0$. The PL decay measurements at 20 and 40 K are composed of PL from Er^{3+} in Si (fast decay) and Er^{3+} in silica (slow decay). For higher temperatures the PL of Er^{3+} in Si quenches and the contribution from Er^{3+} in silica remains.

In order to selectively excite Er^{3+} in either *c*-Si or silica we can make use of their different excitation and quenching mechanisms. To selectively excite Er^{3+} in *c*-Si the excitation wavelength can be tuned off resonance from an Er^{3+} absorption line (e.g., 501 nm). In this case Er^{3+} in silica is not excited, while in *c*-Si photocarriers do excite Er^{3+}. Figure 5

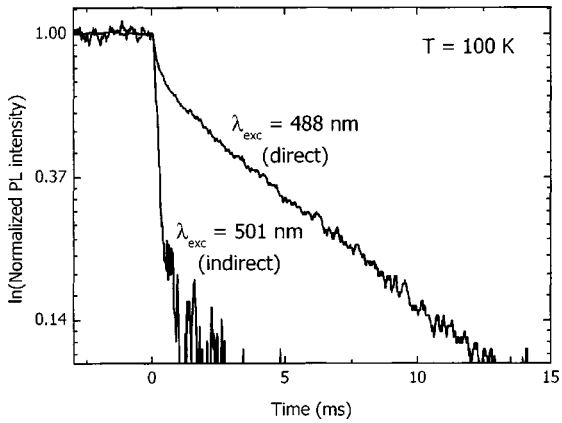

FIG. 5. Normalized PL decay measurements, taken at 1.536 μm and 100 K (see Fig. 3) for two different excitation wavelengths. After excitation at 488 nm the laser is switched of at $t=0$ and the decay curve shows a slow decay contribution from Er^{3+} in silica, together with a fast decay from Er^{3+} in Si. Using indirect excitation (501 nm) only Er^{3+} in Si is excited and the corresponding fast decay component is observed.

TABLE I. Conditions for the selective excitation of Er^{3+} in a Si-infiltrated silica colloidal crystal annealed at 750 °C. Selective excitation can be accomplished by varying the PL temperature and the excitation wavelength.

Origin of PL	PL temperature	Excitation wavelength
Er^{3+} in *c*-Si	low (20 K)	indirect, below electronic band gap wavelength (e.g., 457 nm)
Er^{3+} in silica	high (>200 K)	direct (e.g., 488 nm)
Er^{3+} in *c*-Si and silica	intermediate (100 K)	direct (e.g., 488 nm)

shows normalized time-dependent PL decay measurements at a temperature of 100 K for either direct (488 nm) or indirect excitation (501 nm). At an excitation wavelength of 501 nm we observe only the fast decay of Er^{3+} in *c*-Si. However, at an excitation wavelength of 488 nm we observe a two-component decay with a fast contribution from Er^{3+} in *c*-Si and a slow contribution from Er^{3+} in silica. Consequently, by choosing the appropriate excitation wavelength, we can observe PL from Er^{3+} in *c*-Si only or from Er^{3+} in both *c*-Si and silica. To measure PL from Er^{3+} in silica only, we can now increase the temperature to quench the PL from Er^{3+} in *c*-Si (see Fig. 3). Table I summarizes the various ways Er^{3+} can be excited selectively in *c*-Si and/or silica. Eventually, selective excitation will enable us to probe the DOS selectively in either one of these materials.

Variations in the DOS can be measured by comparing Er^{3+} decay rates in fcc Si-inverted opal PCs with different lattice constants. The Er^{3+} spontaneous emission rate is expected to be fully inhibited in PCs in which the silica is etched out, provided the lattice constant is chosen such that the PBG overlaps with Er^{3+} emission spectrum and the Er ions are implanted deep enough into the photonic crystal. From Fig. 3 we can now determine design criteria for an fcc Si inverted opal PC to obtain a large effect on the spontaneous emission. If we assume full infiltration and a refractive index of 3.5 at a wavelength of 1.5 μm, the calculated PBG bandwidth is 5%[12] (80 nm at 1559 nm). Overlap of the PBG with the Er^{3+} emission spectrum is optimal for a center gap frequency at 1559 nm, which is slightly larger than the Er^{3+} peak emission wavelength. The horizontal bar in Fig. 3 indicates the overlap of the calculated PBG with the Er^{3+} emission spectrum for the case of Er^{3+} in *c*-Si for a center wavelength of 1559 nm. The corresponding lattice parameter for an fcc Si inverted opal is $a=1237$ nm (cubic unit cell), which corresponds to a colloid diameter of 875 nm. It should be noted that the infiltration process often does not lead to a complete Si filling of the interstices within the silica colloidal crystal and, as near-field reflection measurements have shown,[11] this results in an increase of the PBG center frequency. To compensate for this effect, the colloid diameter has to be taken slightly larger, in order to match the PBG with the Er^{3+} emission spectrum. Consequently, precise control over the colloid diameter and refractive index has to be achieved to obtain a PBG that overlaps with the Er^{3+} emission spectrum. However, we note that theoretical work[12] has shown that band gaps for incompletely infiltrated crystals can be as large as 8%, which is well beyond the spectral width observed in Fig. 3.

IV. CONCLUSION

We have shown the successful fabrication of an Er-doped fcc Si inverted opal PC. By annealing the crystal at 400 °C the Er^{3+} ions are activated in the *a*-Si host, but not in silica. An inhomogenously broadened emission spectrum is observed for Er^{3+} in *a*-Si, with a PL lifetime of 300 μs. After annealing at 750 °C Er^{3+} is activated in both Si and silica. The high anneal temperature caused the Si to crystallize and Stark peaks, reflecting the Si crystallization, were observed in the Er^{3+} PL spectrum. The PL lifetime of Er^{3+} in *c*-Si was 0.9 ms, close to the expected radiative lifetime of Er^{3+} in Si. At this anneal temperature Er^{3+} in silica is also activated, and a lifetime of 7 ms is observed. Both in *a*-Si and *c*-Si the Er luminescence quenches with increasing temperature. By varying the PL temperature and the excitation wavelength we can selectively excite Er in Si and/or silica. In future experiments this makes it possible to probe the DOS selectively in either one of these materials. For Er^{3+} in crystalline Si the emission linewidth fits well within the calculated PBG bandwidth. The long emission lifetime of Er in Si, is likely to be close to the radiative lifetime. These characteristics make these PCs ideally suited for experiments demonstrating the effect of the PBG on the spontaneous emission.

ACKNOWLEDGMENTS

Hong Wei is gratefully acknowledged for the refractive index measurements. This work is part of the research program of the ''Stichting voor Fundamenteel Onderzoek der Materie (FOM)'', which is financially supported by the ''Nederlandse organisatie voor Wetenschappelijk Onderzoek (NWO).'' It was also supported in part by the MRSEC Program of the National Science Foundation under Award Number DMR-0212302. Y.J. acknowledges a fellowship from the Industrial Partnership for Research in Interfacial and Materials Engineering at the University of Minnesota.

[1] E. Fermi, Rev. Mod. Phys. **4**, 87 (1932).
[2] E. M. Purcell, Phys. Rev. **69**, 681 (1946).
[3] V. P. Bykov, Sov. J. Quantum Electron. **4**, 861 (1975).
[4] E. Yablonovitch, Phys. Rev. Lett. **58**, 2059 (1987).
[5] S. John, Phys. Rev. Lett. **58**, 2486 (1987).
[6] A. F. Koenderink, L. Bechger, H. P. Schriemer, A. Lagendijk, and W. L. Vos, Phys. Rev. Lett. **88**, 143903 (2002).
[7] M. J. A. de Dood, A. Polman, and J. G. Fleming, Phys. Rev. B **67**, 115106 (2003).
[8] A. Imhof and D. J. Pine, Nature (London) **389**, 948 (1997).
[9] J. E. G. J. Wijnhoven and W. L. Vos, Science **281**, 802 (1998).
[10] A. Blanco *et al.*, Nature (London) **405**, 437 (2000).
[11] Y. A. Vlasov, X. Bo, J. C. Sturm, and D. J. Norris, Nature (London) **414**, 289 (2001).
[12] K. Busch and S. John, Phys. Rev. E **58**, 3896 (1998).
[13] W. Stöber, A. Fink, and E. Bohn, J. Colloid Interface Sci. **26**, 62 (1968).
[14] H. Giesche, J. Eur. Ceram. Soc. **14**, 205 (1994).
[15] P. Jiang, J. F. Bertone, K. S. Hwang, and V. L. Colvin, Chem. Mater. **11**, 2132 (1999).
[16] M. Doosje, B. J. Hoenders, and J. Knoester, J. Opt. Soc. Am. B **17**, 600 (2000).
[17] Y. A. Vlasov, M. Deutsch, and D. J. Norris, Appl. Phys. Lett. **76**, 1627 (2000).
[18] L. H. Slooff, M. J. A. de Dood, A. van Blaaderen, and A. Polman, Appl. Phys. Lett. **76**, 3682 (2000).

[19] J. H. Shin, R. Serna, G. N. van den Hoven, A. Polman, W. G. J. H. M. van Sark, and A. M. Vredenberg, Appl. Phys. Lett. **68**, 997 (1996).
[20] P. G. Kik, M. J. A. de Dood, K. Kikoin, and A. Polman, Appl. Phys. Lett. **70**, 1721 (1997).
[21] N. Hamelin, P. G. Kik, J. F. Suyver, K. Kikoin, A. Polman, A. Schönecker, and F. W. Saris, J. Appl. Phys. **88**, 5381 (2000).
[22] J. S. Custer, E. Snoeks, and A. Polman, Mater. Res. Soc. Symp. Proc. **235**, 51 (1992).
[23] S. Coffa, G. Franzó, F. Priolo, A. Polman, and R. Serna, Phys. Rev. B **49**, 16313 (1994).
[24] M. J. A. de Dood, P. G. Kik, J. H. Shin, and A. Polman, Mater. Res. Soc. Symp. Proc. **422**, 219 (1996).
[25] J. S. Custer, A. Polman, and H. M. van Pinxteren, J. Appl. Phys. **75**, 2809 (1994).
[26] M. J. A. de Dood, L. H. Slooff, A. Moroz, A. van Blaaderen, and A. Polman, Phys. Rev. A **64**, 033807 (2001).
[27] A. Polman, G. N. van den Hoven, J. S. Custer, J. H. Shin, R. Serna, and P. F. A. Alkemade, J. Appl. Phys. **77**, 1256 (1995).